JPE 15-5-23

http://dx.doi.org/10.6113/JPE.2015.15.5.1367
ISSN(Print): 1598-2092 / ISSN(Online): 2093-4718

Investigation of a Hybrid HVDC System with DC Fault Ride-Through and Commutation Failure Mitigation Capability

Chunyi Guo†, Chengyong Zhao*, Maolan Peng**, and Wei Liu*

†,*State Key Laboratory for Alternate Electrical Power System with Renewable Energy Sources, North China Electric Power University, Beijing, China
**Maintenance and Test Center of Extra High Voltage Power Transmission Company of China Southern Power Grid Co., Ltd, Guangzhou, China

Abstract

A hybrid HVDC system that is composed of line commutated converter (LCC) at the rectifier side and voltage source converter (VSC) in series with LCC at the inverter side is studied in this paper. The start-up strategy, DC fault ride-through capability, and fault recovery strategy for the hybrid HVDC system are proposed. The steady state and dynamic performances under start-up, AC fault, and DC fault scenarios are analyzed based on a bipolar hybrid HVDC system. Furthermore, the immunity of the LCC inverter in hybrid HVDC to commutation failure is investigated. The simulation results in PSCAD/EMTDC show that the hybrid HVDC system exhibits favorable steady state and dynamic performances, in particular, low susceptibility to commutation failure, excellent DC fault ride-through, and fast fault recovery capability. Results also indicate that the hybrid HVDC system can be a good alternative for large-capacity power transmission over a long distance by overhead line.

Key words: Commutation failure, DC fault ride-through, hybrid HVDC, Line commutated converter, Voltage sourced converter

I. INTRODUCTION

At present, the line commutated converter-based high voltage direct current (LCC-HVDC) system has been widely used in many areas, such as asynchronous ac grid connection, long-distance bulk power transmission, etc. [1]. However, LCC-HVDC has some inherent disadvantages that limit its application to some extent. The minimum required short circuit ratio (SCR) for LCC is limited, thus, if the SCR of AC network is low, LCC-HVDC would have poor voltage regulation ability and be susceptible to commutation failures (CFs). In the multi-infeed HVDC system, cascaded CFs will significantly affect the security and stability of system operation [2]. Recently, voltage source converters have become a viable alternative for HVDC transmission (VSC-HVDC). These converters have many advantages such as the ability to operate in very weak AC networks, no CF issue, reduced harmonics, and good controllability [3]-[5]. Particularly, modular multilevel converter (MMC), a VSC topology, draws more interest because of its scalability and modularity properties, lower losses, and potential application in high-voltage and large-capacity transmission areas [6]-[8]. However, capital cost and losses of VSC-HVDC are higher than LCC-HVDC, and the voltage and power ratings are relatively lower [9]. Hence, the hybrid HVDC system that integrates LCC-HVDC and VSC-HVDC will be beneficial. There are many types of hybrid HVDC schemes. A hybrid multi-infeed system is proposed [10], and an index of "apparent increase in short circuit ratio" (AISCR) is used to measure the effect of a VSC-HVDC infeed on LCC-HVDC at the same busbar. The LCC-VSC type

Manuscript received Apr. 16, 2015; accepted Jun. 10, 2015
Recommended for publication by Associate Editor Kyeon Hur.
†Corresponding Author: chunyiguo@outlook.com
Tel: +86-10-61773741, Fax: +86-10-61773744, North China Electric Power University
*State Key Laboratory for Alternate Electrical Power System with Renewable Energy Sources, North China Electric Power Univ., China
**Maintenance and Test Center of Extra High Voltage Power Transmission Company of China Southern Power Grid Co., Ltd, China

hybrid HVDC system [11] and LCC-HVDC with STATCOM infeed [12] were also investigated. The main purpose of these hybrid HVDC systems is to reduce the commutation failure risks of LCC with the support of VSC. However, the DC fault ride-through capability is always an issue, as illustrated below.

In China, an existing Tianshengqiao-Guangzhou LCC-HVDC project (±500 kV, 1800MW) is considered to be reconstructed by China Southern Power Grid (CSG) to improve the receiving side AC voltage regulation ability and reduce CF probability of the LCC inverter. One option is to replace the LCC inverter with VSC. However, the overhead transmission line with a length of 960 km will be preserved. Thus, DC faults are inevitable for long-distance power transmission with overhead line, and it will be an enormous challenge for VSC in hybrid HVDC system to ride-through DC faults. Currently used methods trip AC circuit breaker or employ DC breaker. However, the recovery time of VSC from DC fault is longer once the AC circuit breaker trips, and the DC breaker is costly and not mature enough to be applied [13], [14]. The MMC with full-bridge submodules (FBSMs) and clamp double submodules (CDSMs) are feasible options to ride-through the DC faults [15], [16]. Relevant and similar topologies are reported on ride-through the DC fault. An alternate arm converter (AAC) topology [17] is a hybrid converter with FBSM-based MMC and two-level converter. The modulation and control strategies [19] of a new hybrid VSC with DC fault-tolerant capability called hybrid cascaded multilevel converter (HCMC) [18] are further studied. A new sub-module structure was also proposed [20]. A common disadvantage of these topologies is the need for massive power electronic devices that lead to higher costs. Therefore, a hybrid HVDC system with DC fault ride-through and CFs mitigation capabilities, as well as lower capital costs, will be highly valued in the research and engineering of large-power and long-distance transmission areas.

Based on the LCC-MMC scheme, a diode group is applied on a DC line to block the DC fault current between MMC and fault location [21]. However, the power loss of diodes at a steady-state operation is a considerable issue. A technical feasibility study of diode–rectifier and VSC inverter-based HVDC Link for offshore wind farms is proposed, loss analysis is carried out, and good fault ride-through performances to solid faults are obtained [22]. In addition, a distributed protection strategy has been designed, so each wind turbine reacts to the different faults using mainly local measurements. In [23], a hybrid HVDC with LCC and VSC in series as inverter is presented, and a control system and its dynamic performance under AC fault conditions are investigated. However, system performances under DC fault condition and fault recovery control method are not fully analyzed. A novel converter topology consisting of a series connection of 12-pluse diode rectifiers and VSC is proposed [24] for integrating an offshore wind farm with reduced cost and power loss. The dynamic performances under changing load and AC grid fault are investigated. A converter suitable for large-scale integration of wind power directly through HVDC is presented [25]. The topology and its control strategy including black start, reversing power flow, and DC fault rid-through are validated. However, the CF issue of LCC at the inverter side needs to be further studied.

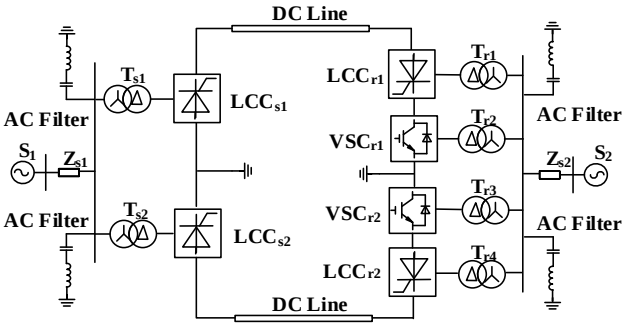

Fig. 1. Schematic diagram of the hybrid HVDC System.

In this paper, a hybrid HVDC with LCC as rectifier and VSC in series with LCC as inverter are further examined. First, the structure and control scheme of the hybrid HVDC are presented. The start-up strategy, DC fault ride-through capability, and fault recovery method for the hybrid HVDC system are proposed. The system performances under start-up, steady-state, AC fault, and DC fault conditions are investigated in PSCAD/EMTDC. Moreover, the CF immunity of the LCC inverter in the hybrid HVDC is analyzed and compared with comparable LCC-HVDC. The results show that the hybrid HVDC system exhibits favorable operation performances, particularly, DC fault ride-through, CF mitigation, and fast recovery.

II. THE HYBRID HVDC SYSTEM

Fig. 1 illustrates a bipolar hybrid HVDC system. S_1 and Z_{s1} are the equivalent sending AC system and impedance, respectively. S_2 and Z_{s2} are the equivalent receiving ac system and impedance, respectively. The positive pole is identical with the negative pole. The rectifier is composed of LCC converters (LCC_{s1} and LCC_{s2}). The inverter adopts the LCC (LCC_{r1} and LCC_{r2}) in series with VSC (VSC_{r1} and VSC_{r2}). The hybrid HVDC system also includes converter transformers T_{s1} and T_{s2} at the sending side, transformers T_{r1}, T_{r2}, T_{r3}, and T_{r4} at the receiving side, DC lines, and filters. For VSC at the inverter side, the half-bridge MMC [6] is applied. The VSC can provide the necessary reactive power and commutation voltage support for LCC at the inverter side, and transmit some amount of active power.

The series hybrid inverter of the positive pole in the hybrid

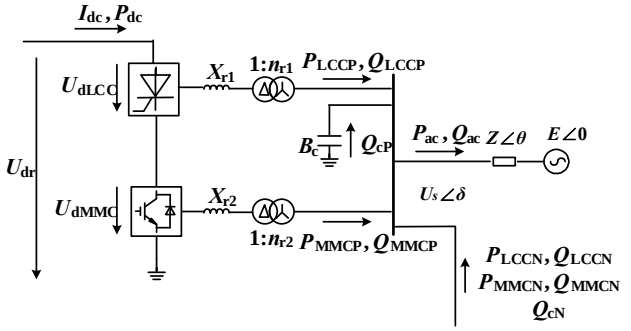

Fig. 2. The series hybrid inverter scheme of one pole.

HVDC system, as shown in Fig. 2, integrates the MMC and LCC converters in series.

The system parameters are defined as follows:

P_{dc}, I_{dc}: DC real power and current;

U_{dr}: Unipolar DC voltage of inverter;

U_{dLCC}, U_{dMMC}: DC voltage of LCC and MMC;

X_{r1}, n_{r1}: transformer leakage reactance and turn ratio for LCC;

X_{r2}, n_{r2}: transformer leakage reactance and turn ratio for MMC;

P_{LCCP}, Q_{LCCP}: active and reactive power transmitted by LCC of the positive pole;

P_{MMCP}, Q_{MMCP}: active and reactive powers transmitted by MMC of the positive pole;

B_c,Q_{cP}: Equivalent admittance and reactive power of the filters and compensator for LCC of the positive pole;

P_{LCCN}, Q_{LCCN}: active and reactive power transmitted by LCC of the negative pole;

P_{MMCN}, Q_{MMCN}: active and reactive powers transmitted by MMC of the negative pole;

Q_{cN}: Equivalent reactive power of the filters and compensator for LCC of the negative pole;

P_{ac}, Q_{ac}: active and reactive power transmitted to AC system;

$U_s\angle\delta$: Line to line voltage at AC busbar;

$Z\angle\theta$: system equivalent impedance;

$E\angle 0$: electromotive force (emf).

Based on Fig. 2, the following power flow equations can be obtained, supposing that MMC and LCC have the same DC voltage ratings.

$$U_{dLCC} = 2\times\left(\frac{3\sqrt{2}U_s}{\pi n_{r1}}\cos\alpha - \frac{3}{\pi}X_{r1}I_{dc}\right) \quad (1)$$

$$P_{LCCP} = U_{dLCC}I_{dc} \quad (2)$$

$$Q_{LCCP} = P_{LCCP}\tan\phi \quad (3)$$

$$\cos\phi = -[\cos\gamma + \cos(\gamma+\mu)]/2 \quad (4)$$

$$Q_{cP} = B_c U_s^2 \quad (5)$$

$$U_{dLCC} = U_{dMMC} \quad (6)$$

$$U_{sMMC}(t) = \frac{1}{2}mU_{dMMC}\sin(\omega t + \Delta\delta) \quad (7)$$

$$P_{MMCP} = \frac{U_s m U_{dMMC}\sin\Delta\delta}{2n_{r2}X_{r2}} \quad (8)$$

$$Q_{MMCP} = \frac{U_s(mU_{dMMC}\cos\Delta\delta - 2U_s)}{2n_{r2}X_{r2}} \quad (9)$$

$$P_{ac} = \frac{U_s^2\cos\theta - EU_s\cos(\theta+\delta)}{Z} \quad (10)$$

$$Q_{ac} = \frac{U_s^2\sin\theta - EU_s\sin(\theta+\delta)}{Z} \quad (11)$$

$$U_{dLCC} + U_{dMMC} = U_{dr} \quad (12)$$

$$P_{LCCP} + P_{MMCP} + P_{LCCN} + P_{MMCN} = P_{ac} \quad (13)$$

$$Q_{LCCP} + Q_{MMCP} + Q_{cP} + Q_{LCCN} + Q_{MMCN} + Q_{cN} = Q_{ac} \quad (14)$$

where μ and γ are the commutation overlap angle and extinction angle, respectively; $U_{sMMC}(t)$ and $\Delta\delta$ are the fundamental components of AC output voltage of MMC and the phase angle difference between the MMC output voltage and busbar voltage, respectively; m is the modulation index of MMC. Here, the nominal DC voltages of LCC and MMC are identical, and the calculation of power flow from the negative pole (P_{LCCN}, Q_{LCCN}, P_{MMCN}, Q_{MMCN} and Q_{cN}) is same with that of positive pole. Based on the equations above, the control strategies of hybrid HVDC are designed, and dynamic performances under faults condition are analyzed.

III. CONTROL STRATEGY

For the hybrid HVDC system, the DC current control and DC voltage control are utilized for the rectifier and inverter, respectively. Both the LCC and VSC converters in series at the inverter side will control the DC voltage. With the integration and minor improvement of the existing control strategies for LCC and VSC, the control methods for the hybrid HVDC system can be derived as follows.

A. Control Strategy for LCC and VSC

1) LCC Control Strategy: The LCC control strategies of two poles are identical, and the control system is shown in Fig. 3. At the rectifier side, based on Eqs. (1) and (2), constant DC current control and minimal firing angle control are applied. For the LCC at the inverter, constant DC voltage control is utilized, and constant extinction angle and DC current control are also implemented as the backup control.

A novel voltage error control (VEC) is proposed, and implemented together with current error control (CEC) to make the transition smooth among the different control modes, i.e., the constant extinction angle, DC current, and DC voltage control. Thus, the control strategy can avoid frequent switching among different control modes. In addition, voltage dependent current order limiter (VDCOL) is also utilized. Here, the function of the presented VEC is similar with that of the existing CEC. Adding a smooth transition could result in a more gradual change. VEC is achieved by increasing γ (extinction angle) signal in proportion to the DC voltage error.

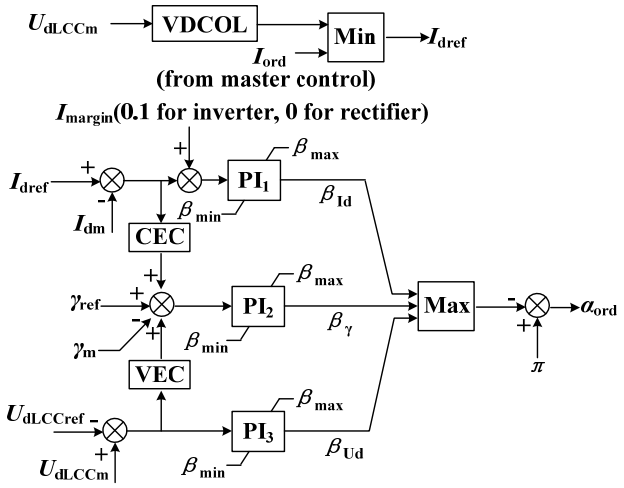

Fig. 3. LCC control system.

The increment is only added when the DC voltage is smaller than the reference value. In the simulation case in Section IV, the proportion gain of VEC is set to 5 degrees/0.1pu to investigate the presented hybrid HVDC system and its control method.

2) MMC Control Strategy: The MMC controller in dq reference frame includes inner current control and outer control [26], as shown in Fig. 4.

B. Start-Up Strategy

The nominal voltages of LCCs at the rectifier and inverter sides are different and MMC is in series with LCC at the inverter side, hence an effective start-up strategy is essential to achieve a secure and stable start-up of the hybrid HVDC system.

The traditional two-stage start-up scheme, i.e., uncontrolled rectifier stage and constant DC voltage control stage, is implemented for the MMC start-up [27].

During the MMC start-up process, the LCCs at both sides are blocked. When the DC voltage of the MMC reaches the rated value, the LCCs are de-blocked, and the current at the rectifier side and the voltage at the inverter side ramps up to the rated values, respectively. The start-up methods of both poles are same, thus, only the start-up procedure of one pole is presented as follows:

1) All the converters are blocked, and SMs in MMC are charged by the receiving AC system. The current-limiting resistance is employed to limit the charging current.
2) With the resistance disconnected, MMC is de-blocked and the DC voltage control is activated.
3) After the DC voltage of MMC reaches the rated value, the LCCs are de-blocked at both sides and control the DC current and DC voltage increases to the rated value. This process is similar with that of LCC-HVDC.

C. DC Fault Ride-Through and Recovery Control Strategy

1) DC Fault Ride-Through Capability: When pole-to-ground DC fault occurs, the LCC at the rectifier side can withstand the temporary over-current, and the temporary over-current can be reduced by force retard control.

To analyze the short-circuit pathway at the inverter side, an equivalent circuit of one pole is shown in Fig. 5. For MMC, the short-circuit current can be caused by two reasons under the DC fault condition: the discharging of capacitors in SMs and the AC system through the freewheeling diodes. However, the short circuit pathway of the series hybrid inverter under DC fault is blocked by the LCC part in the inverter because of the unilateral conductivity of the thyristors, as shown in Fig. 5. Thus, the hybrid series inverter can block the DC fault current effectively.

2) Recovery Control Strategy: The DC fault current of the inverter is blocked by the LCC part, thus the capacitors in SMs will not be discharged, which hastens the recovery of the system from the fault. The recovery control strategy for the hybrid HVDC system is essentially the same with the start-up method. After clearing the DC fault, the DC voltage of MMC can be quickly recovered to its rated value by constant DC voltage control because capacitor charging progress is not required. The LCC current at the rectifier side and the LCC voltage at the inverter side both reach the rated values by their controllers. Finally, the hybrid HVDC recovers to its normal operation state.

From the analysis above, the hybrid HVDC system in this paper will be a good alternative for large-capacity power transmission over a long distance with overhead line, such as the reconstruction project of Tianshengqiao-Guangzhou LCC-HVDC. However, it is difficult to reverse power flow, and this issue will be discussed later.

D. Discussion of Optional Methods to Reverse the Power

In the hybrid HVDC system in this paper, power reversal is a crucial issue. Generally, the system would be applied for unidirectional power flow situations, such as the west-east electricity transmission projects in China. If the power reversal is required, the following methods can be adopted. The corresponding detailed procedures will be studied in future.

Scheme 1: The polarity reversal of LCC is realized by auxiliary switches to achieve power reversal for the black-start of the hybrid four-terminal HVDC system [28]. Employing a similar method, the polarity of MMC in the inverter of the hybrid HVDC in this paper can also be reversed by auxiliary switches. The operation mode of the LCC at the receiving end from an inverter to a rectifier is changed, as well as the LCC at the sending end from a rectifier to an inverter. Thus, the power of the hybrid HVDC would be reversed. However, capital cost will increase because of the auxiliary switches.

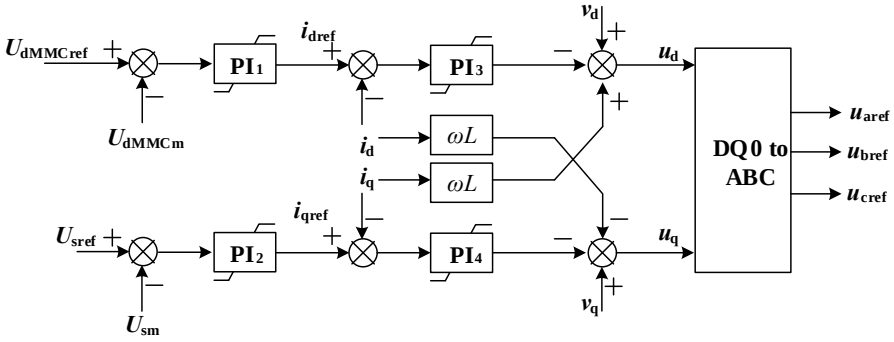

Fig. 4. MCC control system.

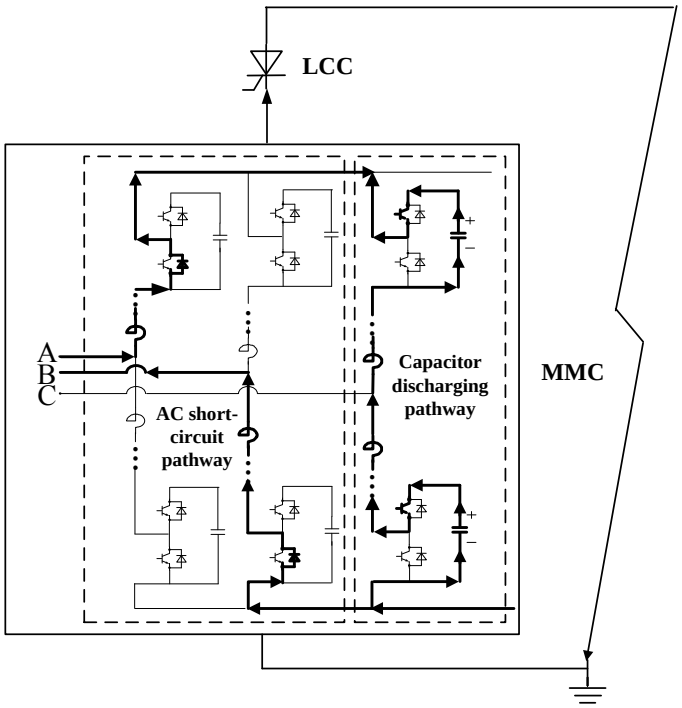

Fig. 5. Inverter equivalent circuit under DC fault condition.

Scheme 2: The full-bridge MMC can change the polarity easily, thus, if the full-bridge type MMC converter series with LCC is implemented at the inverter of the hybrid HVDC system, power can also be reversed.

Scheme 3: Both the rectifier and inverter adopt the series hybrid converter shown in Fig. 2, and the hybrid HVDC can reverse partial power using the MMC converter by bypassing the LCC converters [25].

IV. Simulation Results

To evaluate the hybrid HVDC system, the system performances under start-up, steady-state, AC fault, and DC fault conditions are investigated.

A. Description of the Test System

A bipolar hybrid HVDC system is taken as the test system, as shown in Fig. 1. The rated power and DC voltage of this system are 2000MW and ±500kV, respectively. The system parameters of one pole are shown in Tables I and II.

TABLE I
Parameters of LCC Converters

Items	LCC at rectifier side	LCC at inverter side
AC system voltage U_S	380 kV	212 kV
SCR	2.5	2.5
Transformer capacity S_{TN}	603.73 MVA	591.79 MVA
Transformer ratio K	345/203 kV	230/100.55 kV
Transformer leakage inductance L_t	0.18 p.u.	0.18 p.u.
Reactive compensation capacity Q_c	625 Mvar	312 Mvar
DC voltage U_d	500 kV	250 kV
Rated active power P_d	1000 MW	500 MW

B. Start-up and Steady-state Performance

TABLE II
SYSTEM PARAMETERS OF MMC

Items	Values
Transformer capacity S_{TN}	600 MVA
Transformer ratio K	230/140 kV(Y_0/Δ)
Transformer leakage inductance L_t	11 mH
Arm inductance L	22 mH
DC voltage U_{dc}	250 kV
Rated active power P_d	500 MW
SM capacitance C_0	5 mF
SM capacitor voltage U_C	12.5 kV
Number of SMs N	20(21-level)

The start-up strategy mentioned in Part B of Section III is adopted, and the current-limiting resistance is 35 Ω. Fig. 6 shows the start-up and steady state performances of the positive pole.

The MMC at the inverter side is charged by the receiving system before 0.2 s. The current-limiting resistance is short-circuited, and the DC voltage of MMC increases to the rated value from 0.2 s to 0.5 s, as shown in Fig. 6(a) and Fig. 6(b). During the start-up period, the overshoot of the MMC DC voltage is less than 10%. At 0.6 s, MMC stabilizes and LCCs are de-blocked. The DC current reference value of the LCC at the rectifier side increases to the rated value by the slope of 20kA/s, as depicted in Fig. 6(c), and the DC voltage reference value of the LCC at the inverter side increased to 250 kV in 0.2 seconds, as shown in Fig. 6(d). The LCC converters at both sides are blocked before 0.6 s, thus, the total DC voltage of the hybrid HVDC system is 0, as indicated in Fig. 6(e), and the DC voltage of the LCC at the inverter side is the opposite value of the DC voltage of MMC before 0.6 s. Hence the initial value of the DC voltage reference value for LCC at the inverter side is set to -250 kV. Fig. 6(f) shows that the AC voltage of receiving system can be maintained at a rated value. The steady-state values of the rectifier firing angle and inverter extinction angle of the LCCs are 15.3° and 18.2°, respectively, as shown in Fig. 6(g). Fig. 6(h) indicated that the active power at the rectifier and inverter sides are all finally stable at 1000 MW. The entire hybrid HVDC system reaches the steady state at 1.5 s, and the favorable performances under start-up and steady state conditions are obtained. The performances of the negative pole are same with that of the positive pole, which are not shown here.

C. Dynamic Performances under AC Side Faults

To study the dynamic system performances, the single-phase to ground fault and three-phase to ground fault at the inverter AC busbar are carried out at 2.0 s and 3.0 s, respectively, and both faults lasted 0.1 seconds. To investigate the immunity of LCC to CFs with MMC in series at the inverter side, the dynamic performances of the hybrid HVDC system are compared to that of the modified LCC-HVDC CIGRE benchmark model with a rated DC voltage and power of ±500kV and 2000MW, respectively [29]. The simulation results under the single-phase and three-phase to ground faults are shown in Fig. 7.

Case 1 (Single-phase to ground fault at the inverter side)

Fig. 7(a) to Fig. 7(e) are the simulation results of the LCC-HVDC for comparison, whereas Fig. 7(f) to Fig. 7(j) are the results of the hybrid HVDC. When inductive fault occurs with 0.9358 H inductance grounded at the inverter AC busbar, the receiving AC voltage of LCC-HVDC drops to 0.822pu, and the extinction angle decreases to 0 along with the commutation failure, as seen in Fig(a) and Fig(b). The DC voltage of the LCC at the inverter side drops close to 0, and the DC current increases suddenly, as depicted in Fig. 7(c) and (d). Fig. 7(e) shows that the maximum active power loss of one pole is approximately 950 MW. However, when the same fault occurs at the inverter AC busbar of the hybrid HVDC, more favorable dynamic performances are exhibited. Fig. 7(g) shows that no commutation failure occurs under the same fault condition. The AC voltage of receiving system, DC voltage and DC current slightly fluctuate, and these parameters can be maintained within the rated value, as shown in Figs. 7(f–i). Thus, with the MMC in series, the CFs of LCC are mitigated effectively at the inverter side.

Case 2 (three-phase to ground fault at the inverter side)

Three-phase to ground inductive fault occurs at 3.0 s with 1.1907 H inductance grounded at the inverter AC busbar. The simulation results are also shown in Fig.7. In Fig. 7(a) and 7(b), the receiving AC voltage of the LCC-HVDC drops to 0.814 pu, and the extinction angle decreases to 0 along with the commutation failure. Consequently, the DC voltage of the LCC at the inverter side drops close to 0, and the DC current increases suddenly as seen in Fig. 7(c) and Fig. 7 (d). Fig. 7(e) shows that the maximum active power loss of one pole is approximately 970 MW. However, when the same fault happens at the inverter AC busbar, no CFs occur for the hybrid HVDC, as shown in Fig. 7(g). The AC voltage of the receiving system, DC voltage, and DC current are maintained within the rated value with slight fluctuations, as seen in Fig. 7(f), Fig. 7(h), and Fig. 7(i). Therefore, MMC improves the CF immunity of LCC in series at the inverter side.

To further investigate the CF immunity of the hybrid HVDC, the commutation failure immunity index (CFII) is adopted to evaluate the susceptibility of the LCC-HVDC system and hybrid HVDC system to CFs. CFII is defined in Equation (15), which is a more effective index for CF risk evaluation [30]:

$$CFII = \frac{Critical\ Fault\ MVA}{P_d} \cdot 100\ (\%) \qquad (15)$$

where Critical Fault MVA is the strength of the most severe fault that the tested system can withstand without experiencing any CF. P_d is the DC power of the converter. The larger CFII value indicates a stronger immunity of a LCC inverter to CFs.

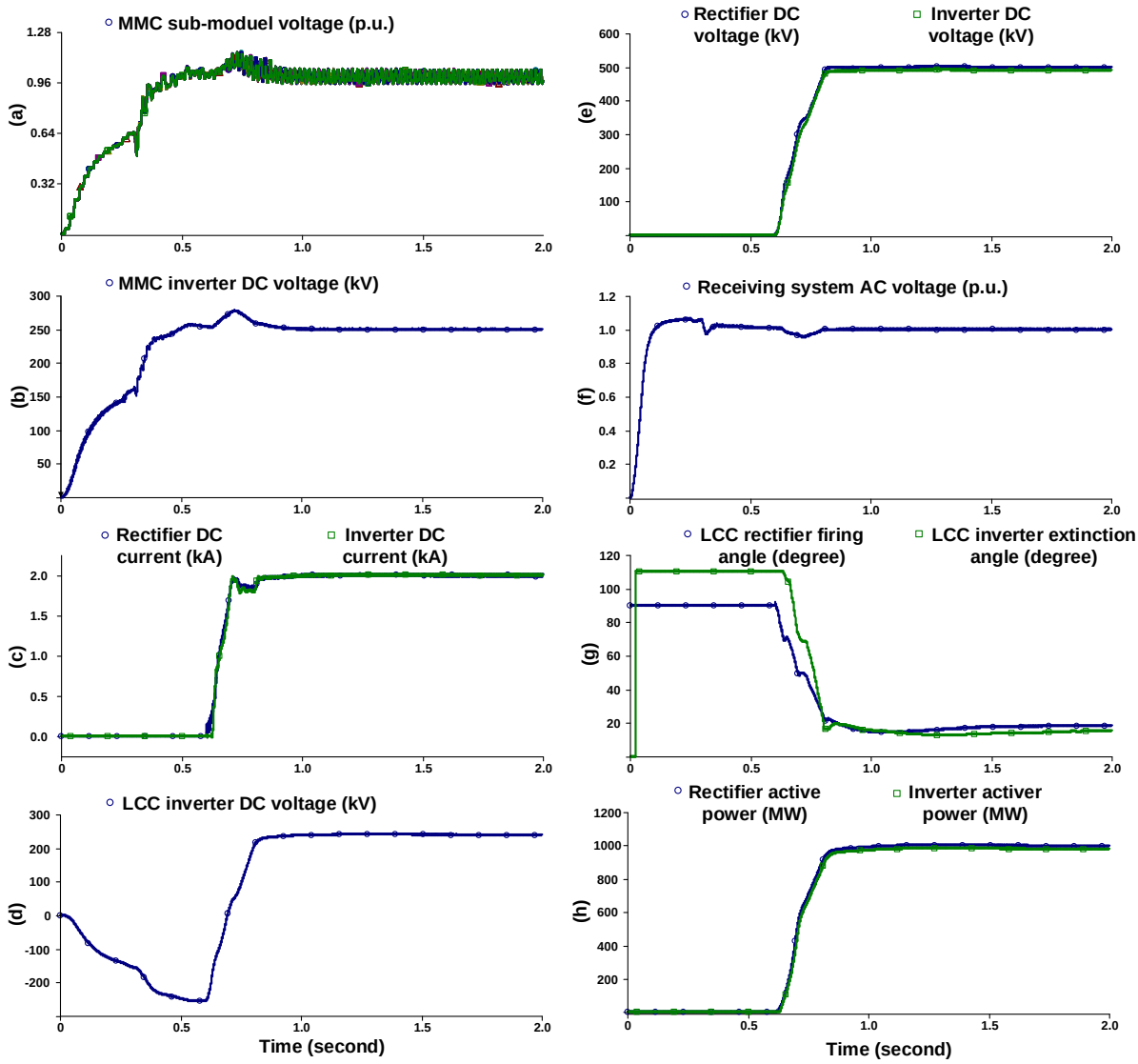

Fig. 6. Simulation results under start-up, steady state condition. (a) MMC sub-moduel voltage. (b) MMC inverter DC voltage. (c) Rectifier and inverter DC current. (d) LCC inverter DC voltage. (e) Rectifier and inverter DC voltage. (f) Receiving system AC voltage. (g) LCC firing angle and extinction angle. (h) Active power.

TABLE III
CFII VALUES OF LCC-HVDC AND HYBRID HVDC

Scenarios	CFII of LCC-HVDC	CFII of hybrid HVDC
Single-phase to ground fault	18.13	32.09
Three-phase to ground fault	14.35	50.20

The CFII values in two different scenarios are considered: 1) single-phase to ground fault and 2) three-phase to ground fault. the results are shown in Table 3.

Based on the results, the larger CFII values are obtained for the hybrid HVDC system, hence the immunity of the LCC inverter to CFs is improved by MMC in the hybrid HVDC system.

D. Dynamic Performances under DC Side Faults

To investigate the DC fault ride-through and recovery capability of the hybrid HVDC system, pole-to-pole fault and single-pole-to-ground fault are applied at 2.0 s. Both faults lasted for 0.2 seconds, and the simulation results are shown in Fig. 8 and Fig. 9.

Case 1 (pole-to-pole fault)

As shown in Fig. 8(a) and (b), when the fault occurs at 2.0 s, the DC voltages at both sides instantly drop to 0 and no active power can be transmitted. However, Fig. 8(c) shows that MMC can still adjust the DC voltage, and the minimum DC voltage is approximately 220 kV during the fault period. Meanwhile, the LCC DC voltage at the inverter side is clamped to the reverse value of the MMC DC voltage, as shown in Fig. 8(d). As the fault occurs, the rectifier side has an over current that is about 1.75 times of the rated DC current value. Meanwhile, the DC fault current at the inverter

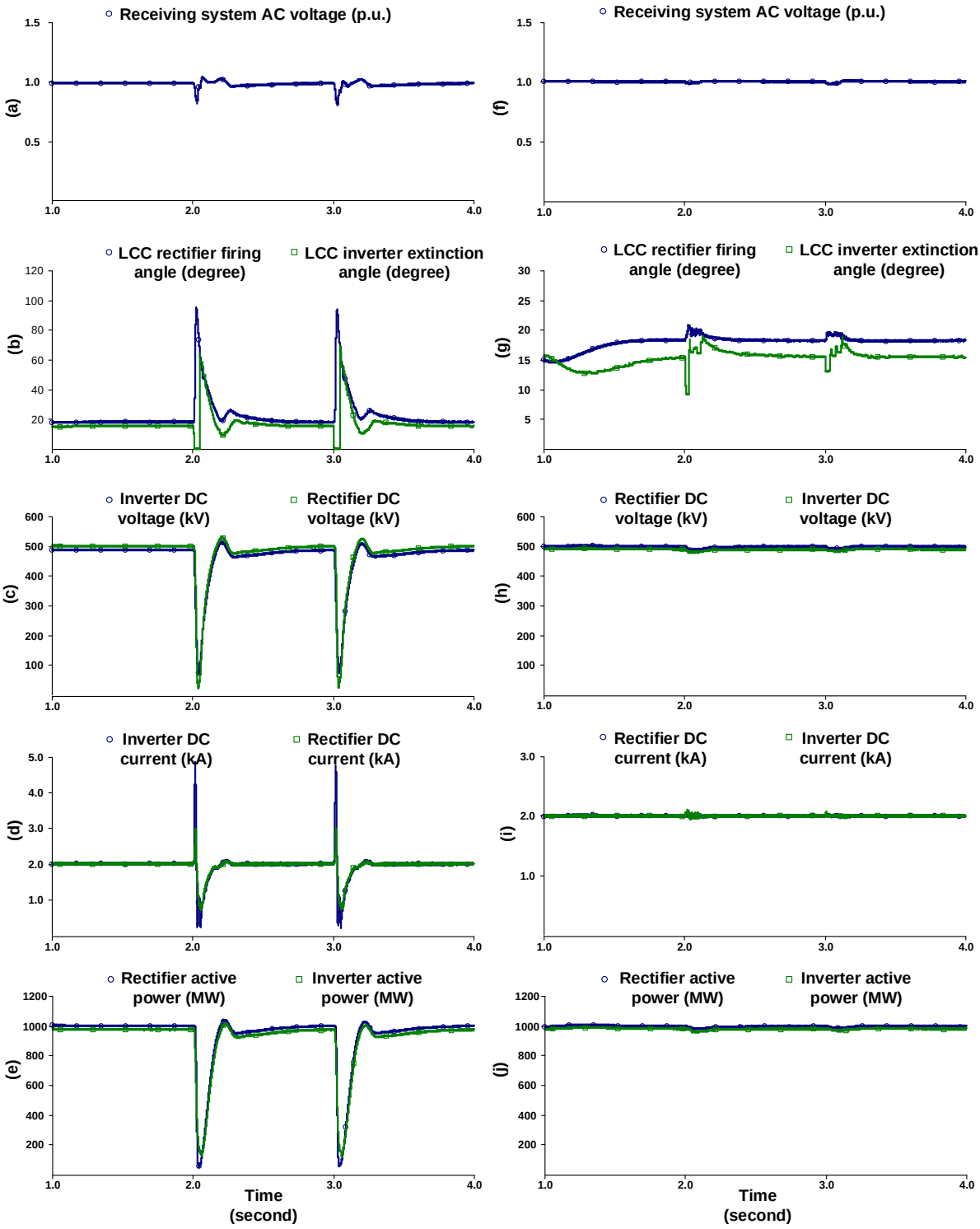

Fig. 7. The simulation results under the single-phase and three-phase to ground faults at the inverter side for the LCC-HVDC and hybrid HVDC. (a) LCC-HVDC receiving system AC voltage. (b) LCC-HVDC rectifier firing angle and rectifier extinction angle. (c) LCC-HVDC DC voltage;(d) LCC-HVDC DC current. (e) LCC-HVDC active power. (f) Hybrid HVDC receiving system AC voltage. (g) Hybrid HVDC rectifier firing angle and inverter extinction angle. (h) Hybrid HVDC DC voltage. (i) Hybrid HVDC DC current. (j) Hybrid HVDC active power.

side is instantly blocked by the LCC part in the inverter, as depicted in Fig. 8(e). Considering a 5 ms fault detection duration, the firing angle of the rectifier is force-retarded to 150°, and the DC fault current can be decreased to 0, as seen in Fig. 8(f). Based on Fig. 8(g), the capacitors in sub-modules are not discharged during the fault, thus, the recovery time of

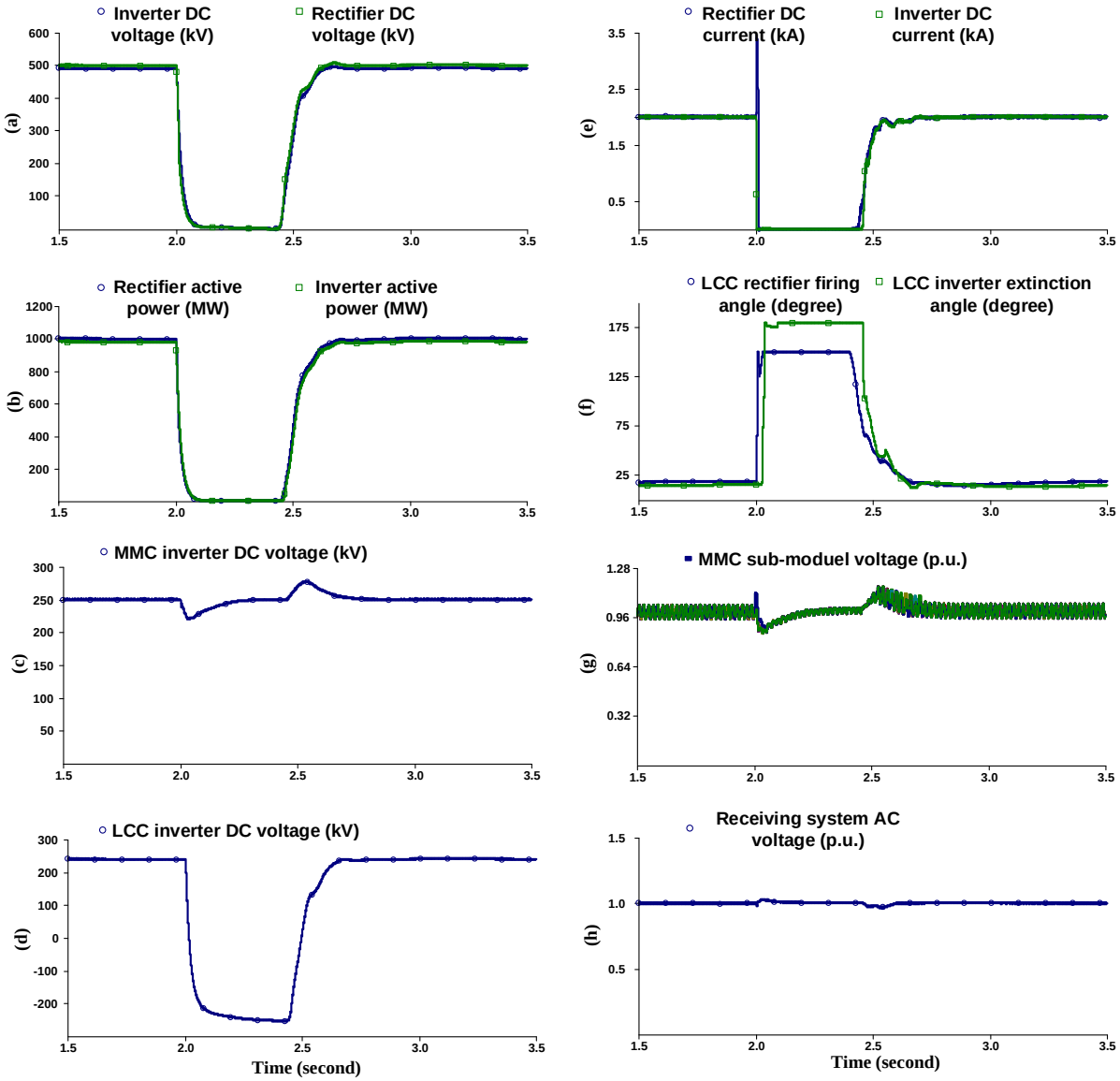

Fig. 8. Simulation results under pole-to-pole fault. (a) Rectifier and inverter DC voltage. (b) Rectifier and inverter active power. (c) MMC inverter DC voltage. (d) LCC inverter DC voltage. (e) Rectifier and inverter DC current. (f) Rectifier firing angle and inverter extinction angle. (g) MMC sub-modules voltage. (h) Receiving system AC voltage.

the hybrid HVDC system from the DC fault shortens.

The fault is cleared at 2.2 s, and the whole system begins to recover at 2.4 s considering the 200 ms of de-energized duration. The following recovery method can be referred in Part C of Section III. During the whole process, the overshoot of the receiving side AC voltage is less than 5%. The hybrid HVDC system reaches the steady state again at 2.8 s. The performances of the negative pole are almost identical with that of the positive pole, which will not be shown here.

Based on Fig. 8, the hybrid HVDC system in this paper can ride-through the pole-to-pole DC fault and exhibits the fast fault recovery capability with the presented control strategy.

Case 2 (single pole-to-ground fault)

At 2.0 s, the positive pole-to-ground fault is applied. In Figs. 9(a–f), the dynamic performances of the positive pole are similar with that under pole-to-pole fault shown in Fig. 8.

When the fault occurs, no active power can be transmitted by the positive pole, seen in Fig. 9(a), and the remaining reactive power compensation for LCC at the positive pole increases AC voltage at the rectifier side. The rectifier firing angle of LCC at the negative pole increases to approximately 40°, as shown in Fig. 9(i), that results in the instantaneous fluctuation of the DC current, as seen in Fig. 9(j). Fig. 9(k) and Fig. 9(l) show that the DC voltage of the negative pole has slight fluctuations. However, after clearing the fault, the hybrid HVDC system can quickly recover to a normal state. During the whole process, the overshoot of the receiving side AC voltage is less than that under pole-to-pole fault. The normal pole still can transmit active power during the single pole-to-ground DC fault. In Fig. 9, the hybrid HVDC system

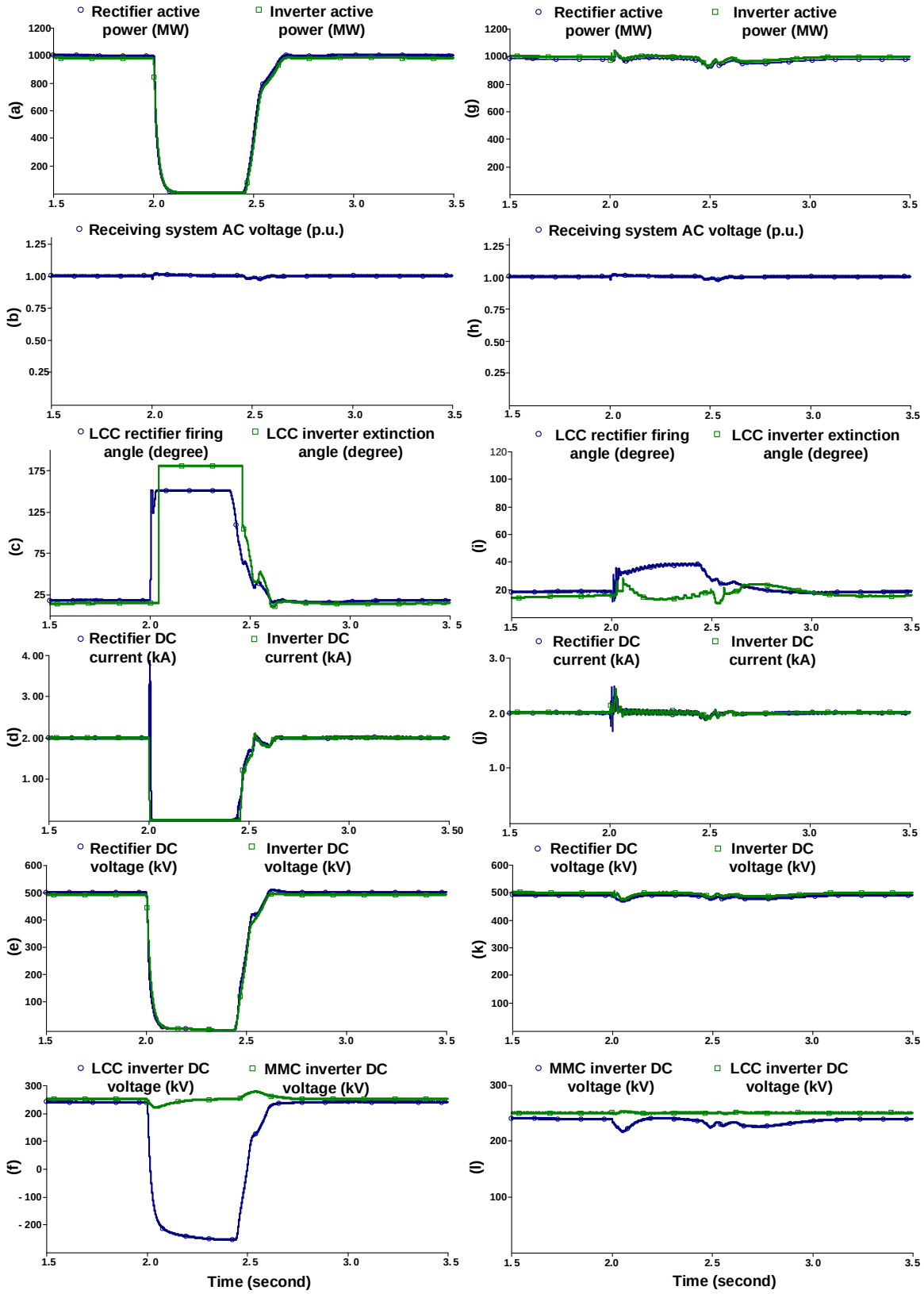

Fig. 9. Simulation results under single pole-to-ground fault. (a) Positive pole active power. (b) Positive pole receiving system AC voltage. (c) Positive pole firing angle and extinction angle. (d) Positive pole DC current. (e) Positive pole DC voltage. (f) Positive pole MMC and LCC inverter DC voltage. (g) Negative pole active power. (h) Negative pole receiving system AC voltage. (i) Negative pole firing angle and extinction angle. (j) Negative pole DC current. (k) Negative pole DC voltage. (l) Negative pole MMC and LCC inverter DC voltage.

can ride-through the single pole-to-ground DC fault and exhibits fast recovery capability with the presented control strategy.

E. Discussion of Nominal DC Voltages of MMC and LCC

For the presented series hybrid HVDC system, the nominal DC voltage of the whole system should be designed after carefully considering the total power capacity, capital cost, and the application scenario, similar to the procedures to determine the DC voltage of conventional LCC-HVDC.

However, the nominal DC voltages of MMC and LCC at the inverter side should de designed considering the following aspects.

1) The nominal DC voltage of the LCC should be higher than or equal to that of the MMC in the inverter. The reasons can be obtained based on Fig. 5 and the case study in Part D in Section IV. During the DC fault condition (both pole-to-pole and pole-to-ground faults), the short circuit pathway of the series hybrid inverter is blocked by the LCC part because of unilateral conductivity of thyristors, as shown in Fig. 5. Thus, the capacitors of SMs in MMC will not be discharged, and the DC voltage of MMC could be adjusted around the rated value during the fault period, as indicated in Figs. 8 and 9. Meanwhile, the LCC DC voltage at the inverter side is clamped to the reverse value of the MMC DC voltage. Thus, if the nominal DC voltage of LCC is less than that of the MMC part, the absolute DC voltage of LCC during the DC fault condition will exceed its nominal value, which adversely affects the LCC converter. Thus, the nominal DC voltage of LCC should be higher than or equal to that of MMC in the inverter.
2) The nominal DC voltage of MMC is one of the key factors of determining power rating for MMC part in the inverter, which will affect the capability of CF mitigation on the LCC part. The main objective of this paper is to investigate the DC fault ride-through and CF mitigation capability of the series hybrid HVDC system. DC voltage is a limitation of MMC rating, hence the CF mitigation effect of MMC on LCC will decline if DC voltage of MMC is designed to a small value that limit reactive power support for AC busbar voltage. Thus, the nominal voltage of MMC could not be small considering the CF mitigation effect.

Hence the nominal DC voltage of MMC and LCC could be designed based on the two aspects above. The nominal DC voltage of MMC and LCC in this paper are identical only for the case study, however, these parameters can be set to other values.

V. CONCLUSIONS

A hybrid HVDC system with LCC as the rectifier and MMC in series with LCC as the inverter is investigated. The control methods for LCC and MMC are introduced. The start-up strategy, DC fault ride-through capability, and fault recovery strategy for the hybrid HVDC system are proposed. Finally, the steady-state and dynamic performances are investigated in PSCAD/EMTDC. Based on the results, the following conclusions can be obtained:

1) The hybrid HVDC system can successfully start-up and has excellent steady state performances compared with the presented control strategy.
2) The system exhibits favorable dynamic performances under AC faults, and it can quickly recover from faults to normal operation state.
3) The hybrid HVDC can ride-through the DC fault, and it exhibits fast fault recovery performances.
4) With VSC in series, the immunity of the LCC inverter to CFs is improved significantly.
5) With the DC fault ride-through and CF mitigation capability, the hybrid HVDC presented in this paper will be a good alternative for long-distance and larger-power transmission by overhead line.

ACKNOWLEDGMENT

Project Supported by National Natural Science Foundation of China (51507060), Special Scientific and Research Funds for Doctoral Specialist of Institution of Higher Learning (20130036120006) and Open Fund of State Key Laboratory of Alternate Electrical Power System with Renewable Energy Source (LAPS15002).

REFERENCES

[1] R. Li, S. Bozhko, and G. Asher, "Frequency control design for offshore wind farm grid with LCC-HVDC link connection," *IEEE Trans. Power Electron.*, Vol. 23, No. 3, pp. 1085-1092, May 2008.
[2] C. Guo, Y. Zhang, A. M. Gole, and C. Zhao, "Analysis of dual-infeed HVDC with LCC-HVDC and VSC-HVDC," *IEEE Trans. Power Del.*, Vol. 27, No. 3, pp. 1529-1537, Jul. 2012.
[3] N. Flourentzou, V. G. Agelidis, and G. D. Demetriades, "VSC-based HVDC power transmission systems: An overview," *IEEE Trans. Power Electron.*, Vol. 24, No. 3, pp. 592-602, Mar. 2009.
[4] C. Guo and C. Zhao, "Supply of an entirely passive AC network through a double-infeed HVDC system," *IEEE Trans. Power Electron.*, Vol. 25, No. 11, pp. 2835-2841, Nov. 2010.
[5] C. Du, E. Agneholm, and G. Olsson, "Comparison of different frequency controllers for a VSC-HVDC supplied system," *IEEE Trans. Power Del.*, Vol. 23, No. 4, pp. 2224-2232, Oct. 2008.
[6] A. Lesnicar and R. Marquardt, "An innovative modular multilevel converter topology suitable for a wide power range," *IEEE Bologna Power Tech Conf.*, 2003.

[7] M. Glinka and R. Marquard. "A new AC/AC multilevel converter family," *IEEE Trans. Ind. Electron.*, Vol. 52, No. 3, pp. 662- 669, Jun. 2005.
[8] S. Rohner, S. Bernet, M. Hiller, and R. Sommer, "Modulation, losses, and semiconductor requirements of modular multilevel converters," *IEEE Trans. Ind. Appl.*, Vol. 57, No. 8, pp. 2633-2642, Aug. 2010.
[9] N. B. Negra, J. Todorovic, and T. Ackermann, "Loss evaluation of HVAC and HVDC transmission solutions for large offshore wind farms," *Elect.Power Syst. Res*., Vol. 76, No. 11, pp. 916-927, Jul. 2006.
[10] C. Guo, Y. Zhang, A. M. Gole, and C. Zhao. "Analysis of dual-infeed HVDC with LCC-HVDC and VSC-HVDC," *IEEE Trans. Power Del.*, Vol. 27, No. 3, 1529-1537, Jul. 2012.
[11] Z. Zhao and M. R. Iravani, "Application of GTO voltage source inverter in a hybrid HVDC link," *IEEE Trans. Power Del.*, Vol. 9, No. 1, pp. 369-377, Jan. 1994.
[12] B. R. Andersen and L. Xu, "Hybrid HVDC system for power transmission to island networks," *IEEE Trans. Power Del.,* Vol. 19, No. 4, pp. 1884-1890, Oct. 2004,
[13] L. X. Tang and B. T. Ooi, "Locating and isolating DC faults in multi-terminal DC systems," *IEEE Trans. Power Del.*, Vol. 22, No. 3, pp. 1877-1884, Jul. 2007.
[14] J. Yang, J. E. Fletcher, and J. O. Reilly, "Short-circuit and ground fault analyses and location in VSC-based DC network cables," *IEEE Trans. Ind. Electron.*, Vol. 59, No. 10, pp. 3827-3837, Oct. 2012.
[15] R. Marquardt, "Modular multilevel converter: An universal concept for HVDC-networks and extended DC-bus-applications," in *Proc. Power Electron. Conf. Int.*, pp. 502-507, 2010.
[16] R. Marquardt, "Modular multilevel converter topologieswith DC-short circuit current limitation," in *Proc. IEEE 8th Int. Conf. Power Electron. ECCE Asia*, pp. 1425-1431, 2011.
[17] M. M. C. Merlin, T. C. Green, P. D. Mitcheson, D. R. Trainer, R. Critchley, W. Crookes, and F. Hassan, "The alternate arm converter: a new hybrid multilevel converter with DC-fault blocking capability," *IEEE Trans. Power Del.*, Vol. 29, No. 1, pp. 310-317, Feb. 2014.
[18] G. P. Adam, S. J. Finney, B. W.Williams, D. R. Trainer, C.D.M. Oates, and D. R. Critchley, "Network fault tolerant voltage-source-converters for high-voltage applications," in *Proc. 9th Int. Conf. AC and DC Power Transmission*, pp. 1-5, 2010.
[19] Y. Xue, Z. Xu, and Q. Tu, "Modulation and control of a new hybrid cascaded multilevel converter with DC blocking capability," *IEEE Trans. Power Del.*, Vol. 27, No. 4, pp. 2227-2237, Oct. 2012.
[20] X. Li, W. Liu, Q. Song, H. Rao, and S. Xu, "An enhanced MMC topology with DC Fault ride-through capability," *IEEE Industrial Electronics Society IECON*, pp. 6182-6188, 2013.
[21] G. Tang, Z. Xu, and Y. Xue, "A LCC-MMC hybrid HVDC transmission system," *Transactions of China Electrotechnical Society*, Vol. 28, No. 10, pp. 301-310, Oct. 2013.
[22] S. Bernal-Perez, S. Ano-Villalba, R. Blasco-Gimenez, and J. Rodriguez-D'Derlee. "Efficiency and fault ride-through performance of a diode-rectifier- and VSC-inverter-based HVDC link for offshore wind farms," *IEEE Trans. Ind. Electron.*, Vol. 60, No. 6, pp. 2401-2409, Jun. 2013.
[23] B. Qahraman and A. M. Gole, "A VSC based series hybrid converter for HVDC transmission," *Electrical and Computer Engineering*, pp. 458-461, May 2005.
[24] T. H. Nguyen, D.-C. Lee, and C.-K. Kim, "A series-connected topology of a diode rectifier and a voltage-source converter for an HVDC transmission system," *IEEE Trans. Power Electron.*, Vol. 29, No. 4, pp. 1579-1584, Apr. 2014.
[25] W. Lin, J. Wen, S. Wang, M. Yao, N. Li, and S. Cheng, "A kind of converters suitable for large-scale integration of wind power directly through HVDC," in *Proc. the CSEE*, Vol. 34, No. 13, pp. 2022-2030, 2014.
[26] M. Guan and Z. Xu, "Modeling and control of a modular multilevel converter-based HVDC system under unbalanced grid conditions," *IEEE Trans. Power Electron*., Vol. 27, No. 12, pp. 4858-4867, Dec. 2013.
[27] L. Tan, Z. Chengyong, X. Jie, C. Xinhong, P. Hui, L. Change, "Start-up scheme for HVDC system based on modular multilevel converter," *IET Renewable Power Generation Conference*, pp. 1-4, 2013.
[28] C. Li, P. Zhan, J. Wen, M. Yao, N. Li, and W.-J. Lee, "Offshore wind farm integration and frequency support control utilizing hybrid multi-terminal HVDC transmission," *IEEE Trans. Ind. Appl.*, Vol. 50, No. 4, pp. 2788-2797, Jul./Aug. 2014.
[29] M. Szechtman, T. Wess, and C. V. Thio, "A benchmark model for HVDC system studies," *1991 IET International Conference on AC and DC Power Transmission*, pp. 374-378, 1991.
[30] E. Rahimi, A. M. Gole, J. B. Davies, I. T. Fernandot, and K. L. Kent, "Commutation failure in single- and multi-infeed HVDC systems," in *Proc. 2006 IEE International Conference on AC and DC Power Transmission*, pp. 182-186, 2006.

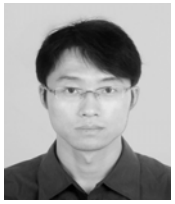

Chunyi Guo was born in Shanxi, China. He received his B.S. and Ph.D degrees in Power System and its Automation in 2007 and 2012 from North China Electric Power University (NCEPU), Beijing, China. At present, he is a lecturer in NCEPU, and also member of CIGRE WG B4.64. His research interests include HVDC and flexible AC transmission systems.

Chengyong Zhao(M'05) was born in Zhejiang, China. He received his B.S., M.S., and Ph.D. degrees in Power System and its Automation from North China Electrical Power University, Beijing, China in 1988, 1993, and 2001, respectively. He is currently the Deputy Director of the Flexible Transmission and Distribution Institute, Electrical and Electronic Engineering School, NCEPU. His research interests include HVDC and flexible AC transmission system.

Maolan Peng was born in Jiangxi, China, in 1991. She received her B.S and M.S. degrees in Power Systems and Automation from North China Electric Power University, Beijing, China in 2012 and 2015, respectively. She is currently working for the Maintenance and Test Center of Extra High Voltage Power Transmission Company of China Southern Power Grid Co., Ltd, Guangzhou, China. Her research field includes HVDC and flexible ac transmission systems.

Wei Liu was born in Zhejiang, China, in 1991. He received his B.S. degree in Automation from North China Electric Power University, Baoding, China in 2013, where he is also currently pursuing his M.Sc. degree in Power System and Automation. His research field includes HVDC and control.